

1 Superiority of chromosomal compared to plasmid-encoded 2 compensatory mutations

3
4 Rosanna C.T. Wright¹ [0000-0002-8095-8256](#), A. Jamie Wood^{2,3} [0000-0002-6119-852X](#), Michael
5 J. Bottery¹ 0000-0001-5790-1756, Katie J. Muddiman¹ [0000-0002-0396-6893](#), Steve Paterson⁴
6 [0000-0002-1307-2981](#), Ellie Harrison⁵ [0000-0002-2050-4631](#), Michael A. Brockhurst¹ [0000-](#)
7 [0003-0362-820X](#), James P.J. Hall^{4*} [0000-0002-4896-4592](#)

- 9 1. Division of Evolution, Infection and Genomic Sciences, University of Manchester,
10 Manchester, United Kingdom
- 11 2. Department of Biology, University of York, York, United Kingdom
- 12 3. Department of Mathematics, University of York, York, United Kingdom
- 13 4. Department of Evolution, Ecology and Behaviour, Institute of Infection, Veterinary and
14 Ecological Sciences, University of Liverpool, Liverpool, United Kingdom
- 15 5. School of Biosciences, University of Sheffield, Sheffield, United Kingdom

16
17 *Correspondence to j.p.j.hall@liverpool.ac.uk

18 19 Abstract

20 Plasmids are important vectors of horizontal gene transfer in microbial communities but can
21 impose a burden on the bacteria that carry them. Such plasmid fitness costs are thought to arise
22 principally from conflicts between chromosomal- and plasmid-encoded molecular machineries,
23 and thus can be ameliorated by compensatory mutations (CMs) that reduce or resolve the
24 underlying causes. CMs can arise on plasmids (i.e. plaCM) or on chromosomes (i.e. chrCM),
25 with contrasting predicted effects upon plasmid success and subsequent gene transfer because
26 plaCM can also reduce fitness costs in plasmid recipients, whereas chrCM can potentially
27 ameliorate multiple distinct plasmids. Here, we develop theory and a novel experimental system
28 to directly compare the ecological effects of plaCM and chrCM that arose during evolution
29 experiments between *Pseudomonas fluorescens* SBW25 and its sympatric mercury resistance
30 megaplasmid pQBR57. We show that while plaCM was predicted to succeed under a broader
31 range of parameters in mathematical models, experimentally chrCM dominated under all
32 conditions, including those with numerous recipients, due to a more efficacious mechanism of
33 compensation, and advantages arising from transmission of costly plasmids to competitors

34 (plasmid ‘weaponisation’). We show analytically the presence of a mixed Rock-Paper-Scissors
35 regime for plaCM, driven by trade-offs with horizontal transmission, that explains the observed
36 failure of plaCM to dominate even in competition against an uncompensated plasmid. Our
37 results reveal broader implications of plasmid-bacterial evolution for plasmid ecology,
38 demonstrating the importance of compensatory mutations for resistance gene spread. One
39 consequence of the superiority of chrCM over plaCM is the likely emergence in microbial
40 communities of compensated bacteria that can act as ‘hubs’ for plasmid accumulation and
41 dissemination.

42

43 **Background**

44 Conjugative plasmids are important for bacterial evolution. Plasmids transfer niche-adaptive
45 ecological functions between lineages and consequently can drive adaptation and genomic
46 divergence (Finks and Martiny, 2023; Vos et al., 2023; Wein and Dagan, 2020). However,
47 acquiring a new conjugative plasmid is frequently costly for the host cell. Such plasmid fitness
48 costs can arise from a variety of causes, including the metabolic burden of plasmid
49 maintenance, disrupted gene regulation, stress responses, cytotoxicity, and mismatched codon
50 usage (San Millan and MacLean, 2017). The long-term persistence of costly plasmids within
51 bacterial lineages often requires compensatory evolution to negate these fitness costs
52 (Brockhurst and Harrison, 2022). Experimental evolutionary studies have revealed that
53 compensatory mutations (CMs) may occur on the plasmid, or the chromosome, or both
54 replicons (Benz and Hall, 2022; Bottery et al., 2017; Dahlberg and Chao, 2003; De Gelder et al.,
55 2007; Hall et al., 2021, 2019; Harrison et al., 2015; Jordt et al., 2020; Loftie-Eaton et al., 2017;
56 San Millan et al., 2015; Stalder et al., 2017). Such CMs affect a wide range of gene functions,
57 including regulatory genes, helicases, other co-resident mobile genetic elements, or
58 hypothetical genes without known function.

59

60 The fitness cost of a given plasmid in a given host can be ameliorated by alternative CMs
61 affecting distinct genetic targets, sometimes encoded by different replicons, i.e., affecting genes
62 on the chromosome, which we term chrCM, or on the plasmid, which we term plaCM. This
63 phenomenon is exemplified by the common soil bacterium *Pseudomonas fluorescens* SBW25
64 (henceforth ‘SBW25’) and the environmental mercury resistance plasmid pQBR57. Both SBW25
65 and pQBR57 were isolated from sugar beet plants at a field site in Wytham Woods, Oxfordshire,
66 UK in the 1990s (Bailey et al., 1995; Lilley et al., 1996). pQBR57 causes a substantial fitness
67 cost in SBW25 due to a specific genetic conflict with a chromosomal hypothetical gene

68 PFLU4242, inducing a sustained SOS response and the maladaptive expression of
69 chromosomal prophages leading to cell damage (Hall et al., 2021). This costly cellular disruption
70 can be negated by single CMs affecting either PFLU4242 itself or a plasmid-encoded regulator
71 PQBR57_0059. Either CM is sufficient to reduce the fitness cost of pQBR57 and both fix the
72 transcriptional disruption caused by pQBR57 acquisition. For clarity, we refer to SBW25 strains
73 with a loss-of-function mutation in PFLU4242 as SBW25::chrCM to indicate chromosomal CM,
74 and strains with a loss-of-function mutation in PQBR57_0059 as pQBR57::plaCM to indicate
75 plasmid CM. Although both CMs evolved in SBW25 plasmid-carrying populations in potting soil
76 microcosms, they were never observed to co-occur in the same genome, suggesting that there
77 is no added benefit of combining both CMs in the same cell. chrCM can ameliorate the fitness
78 costs of other pQBR plasmids, whereas the benefits of plaCM are transmitted when
79 pQBR57::plaCM transfers by conjugation (Hall et al., 2021, 2019).

80
81 Where alternative CMs exist on the chromosome or the plasmid, existing theory predicts that
82 plaCMs will be superior (Zwanzig et al., 2019). This superiority arises because, unlike chrCMs
83 which are only inherited vertically at cell division, plaCMs are also transmitted horizontally by
84 conjugation. Provided the plaCM also negates the fitness cost of the plasmid in newly formed
85 transconjugant cells, the linkage of the plasmid and the CM can thus enhance plasmid
86 maintenance and spread. Correspondingly, plaCMs are predicted to outcompete chrCMs even if
87 plaCMs offer less efficient amelioration than chrCMs. However, previous attempts to explore
88 these predictions theoretically have relied on numerical simulations and extensive parameter
89 fitting (Rebelo et al., 2023a; Zwanzig et al., 2019), limiting the generalisability of the findings,
90 while experimental tests competing alternate modes of CM are lacking altogether. Moreover,
91 some experiments have reported a trade-off between CMs and conjugation rate, which could
92 impede the success of plaCMs (Bethke et al., 2023; Dimitriu et al., 2021; Turner et al., 1998).

93
94 To contrast the effect of chrCM with plaCM on bacteria-plasmid dynamics, we first develop two
95 simple mathematical models based on 3-equation ordinary differential equations (ODEs) in
96 which we consider the arrival of a plasmid-bearing strain with either a chrCM or a plaCM. A key
97 strength of this approach is that the models we create can be solved exactly to provide general
98 understanding. The predictions generated by our models were then tested experimentally. To
99 enable direct competition of chrCM and plaCM we engineered variants of SBW25 and pQBR57
100 carrying defined CMs and fluorescent tags allowing cells containing the plaCM and/or chrCM to
101 be distinguished by flow cytometry. We then performed competition experiments across various

102 ecological scenarios predicted to alter the differential benefits of these contrasting modes of
103 compensatory evolution. Specifically, we varied the strength of mercury selection, the presence
104 of other plasmid replicons in the population, or the availability of plasmid-free recipient cells for
105 onward conjugative transfer within the population. We show that, contrary to expectations,
106 plaCM performs poorly in competition with chrCM under all tested conditions due to lower
107 efficacy of amelioration, a probable trade-off against conjugative efficacy, and an overlooked
108 benefit of chrCM that effectively enables these cells to ‘weaponise’ costly plasmids to reduce
109 the fitness of competitors. Our results have implications for the mobilisation of genes in
110 microbial communities, suggesting that chromosomes are more likely to become plasmid-
111 favourable — and thus hubs of source-sink horizontal gene transfer — than plasmids are to
112 become low-cost generalists across hosts.

113

114 **Results**

115 ***Mathematical model of plasmid- or chromosome-encoded compensatory mutation*** 116 ***dynamics***

117 To understand the dynamics of chrCM and plaCM we modified a simple, well-understood model
118 of bacteria-plasmid population dynamics to include either chrCM or plaCM. Separate models
119 were preferred because the combined system (i.e., containing both chrCM and plaCM) is too
120 complex to solve analytically. The basic model, without CMs, is detailed in the Supplementary
121 Appendix and recapitulated the key findings of previous studies wherein costly plasmids do not
122 invade unless their conjugation rate, γ , is larger than $\mu(\alpha - \beta)/(\alpha - \mu)$, and only competitively
123 displace the plasmid-free population if γ is larger than $\mu(\alpha - \beta)/(\beta - \mu)$, where α is the plasmid
124 free growth rate, β is the plasmid containing growth rate, and μ is the population turnover rate.
125 Positive selection for the plasmid is included via the selection pressure term, η , which is initially
126 set to zero.

127

128 We then considered how the addition of chrCM affects the outcome of this underlying basic
129 system. Here, plasmid free wild-type bacteria (f) and wild-type bacteria containing a wild-type
130 plasmid (p) are invaded by a chrCM variant bearing a wild-type plasmid (c). The compensatory
131 effect is assumed to be imperfect so the growth rate of the three strains are assumed to be α for
132 f , β_p for p , and β_c for c , where $\alpha > \beta_c > \beta_p$. The dynamics of the system are then described by
133 the following set of ODEs:

134

$$\frac{df}{dt} = \alpha f(1 - f - p - c) - \mu f - \gamma_P p f - \gamma_C c f - \eta f \quad (1)$$

$$\frac{dp}{dt} = \beta_P p(1 - f - p - c) - \mu p + \gamma_P p f + \gamma_C c f \quad (2)$$

$$\frac{dc}{dt} = \beta_C c(1 - f - p - c) - \mu c \quad (3)$$

137 In the case of no selection for the plasmid, $\eta = 0$, this set of ODEs can be solved exactly to yield
 138 a simple phase plane structure in which chrCM sweeps to fixation $(0,0,c^*)$ from the expected
 139 stable fixed point of the underlying system according to the value of the conjugation rate (Fig.
 140 1A). When the underlying fixed point is plasmid-free only $(f^*,0,0)$ (i.e. $\gamma_P < \mu(\alpha - \beta_P)/(\alpha - \mu)$) or
 141 mixed $(f^*,p^*,0)$ (i.e. $\mu(\alpha - \beta_P)/(\beta_P - \mu) > \gamma_P > \mu(\alpha - \beta_P)/(\alpha - \mu)$), and compensation is
 142 imperfect, the fixed points are separated by a saddle at (f_s,p_s,c_s) . This means that when the
 143 conjugation rate is sufficiently high the chrCM will always invade, but at lower conjugation rates
 144 (provided $\alpha > \beta_C$) there is a threshold. If the initial proportion of chrCM exceeds the threshold
 145 value (given by the saddle), complete replacement occurs and chrCM successfully invades and
 146 moves to fixation. The reason invasion can occur despite chrCM having lower growth than the
 147 plasmid-free is that a plasmid-carrying chrCM can conjugate the costly plasmid into plasmid-free
 148 competitors, such that chrCM then exceeds the uncompensated competitor's growth rate (i.e.
 149 $\beta_C > \beta_P$) and takes over the system. Selection ($\eta > 0$) reduces the relative ability of plasmid-free
 150 wild-type f to compete against plasmid-bearers, concentrating the dynamics on the competition
 151 between p and c and the difference between β_C and β_Q , thus favouring chrCM. This result is
 152 demonstrated in the Supplemental Appendix, and typically occurs with a linear addition to the
 153 stability conditions which rapidly favour the chrCM plasmid-bearing invader.

154
 155 We next considered a system invaded by a variant bearing a plaCM plasmid (q). This leads to a
 156 set of three differential equations analogous to those above:

$$\frac{df}{dt} = \alpha f(1 - f - p - q) - \mu f - \gamma_P p f - \gamma_Q q f - \eta f \quad (4)$$

159
$$\frac{dp}{dt} = \beta_P p(1 - f - p - q) - \mu p + \gamma_P p f$$
 (5)

160
$$\frac{dq}{dt} = \beta_Q q(1 - f - p - q) - \mu q + \gamma_Q q f$$
 (6)

161 Analysis of the system reveals a more complex phase portrait, described in Fig. 1B in the case
162 of no selection, $\eta = 0$. Consistent with prior work (Zwanzig et al., 2019), comparison of Figs 1A
163 and 1B shows a wider range of conditions in which plaCM is successful compared with chrCM.
164 Where there is no trade-off with conjugation rate, plaCM always displaces the uncompensated
165 plasmid, invading the system if $\gamma_Q < \mu(\alpha - \beta_Q)/(\alpha - \mu)$ and dominating if $\gamma_Q >$
166 $\mu(\alpha - \beta_Q)/(\beta_Q - \mu)$, and, unlike chrCM, in a manner that does not depend on initial conditions.

167
168 Previous experiments have shown that CMs can affect the ability of a plasmid to conjugate
169 (Bethke et al., 2023; Dimitriu et al., 2021; Turner et al., 1998). We therefore investigated how
170 the success of each CM is affected by changes in the conjugation rate. For plaCM, if $\gamma_Q > \gamma_P$,
171 i.e. plaCM confers a higher transfer rate than the wild-type plasmid, the wild-type plasmid is
172 always lost from the system, and the outcome for plaCM collapses into the single-plasmid
173 system described above (Supplementary Appendix). However, if there is a trade-off such that
174 $\gamma_P > \gamma_Q$, various outcomes are possible depending on the other parameters, including loss of
175 both plasmids ($f^*, 0, 0$), fixation of plaCM ($0, 0, q^*$), co-existence between wild-type and plasmid-
176 free ($f^*, p^*, 0$), and, unexpectedly, a state with a stable coexistence between the f , p and q
177 populations (Fig. 1B orange region), which would not be found in a linearised adaptive dynamics
178 approach. The stable fixed point is oscillatory in character (a stable spiral) and is driven by
179 Rock-Paper-Scissors (RPS)-like nontransitive dynamics. When f is large, this promotes the
180 conjugative spread of the fastest conjugating population, p . When p is large, f is small, so the
181 opportunities for conjugation are relatively low but the force of infection remains high due to high
182 γ_P . Here, the q outgrows the p . When q is large opportunities for conjugation are also low but as
183 γ_Q is relatively low the f can outgrow the q . This RPS-like dynamic is approximate as the
184 interactions are not perfectly symmetric: in the prototypical model each type has a direct impact
185 on one other type and is directly impacted by the third. Here the competition arises through a
186 mixture of competitive growth and competitive infection and is different for each combination of
187 subpopulations.

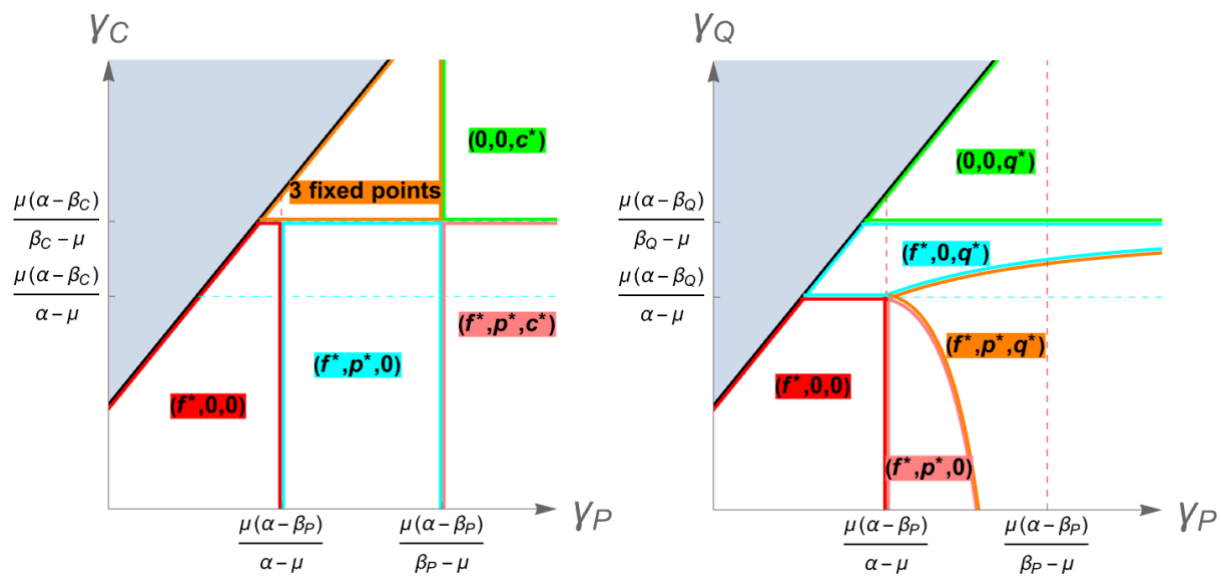
188

189 For chrCM, the system is robust to changes in conjugation rate provided compensation is
 190 sufficiently strong ($\beta_C > \mu(\gamma_C + \alpha)/(\mu + \gamma_C)$). In cases where chrCM has a more substantial
 191 effect on γ_C , the CM is lost (Fig. 1A red and blue regions), except in cases where the
 192 conjugation rate from uncompensated strains is sufficiently high (Fig. 1A pink area, $\gamma_P > \mu(\alpha -$
 193 $\beta_P)/(\beta_P - \mu)$). Under these conditions, the force of infection of costly plasmids ensures that the
 194 frequency of plasmid-bearers in the system is maintained at a high enough level such that
 195 chrCM has sufficient competitive advantage to persist. Although the chrCM system can also
 196 admit an oscillatory stable coexistent solution, driven by a form of RPS dynamics it is only for γ_P
 197 large, γ_C small and further away from the biologically relevant regime.

198

199 Selection simplifies the dynamics of the plaCM system by reducing the effect of the plasmid-free
 200 population (f) to the dynamics. Even when $\gamma_P \gg \gamma_Q$, plaCM is more likely to invade across a
 201 range of parameters because the contribution of the conjugation terms to the dynamic is
 202 reduced, resulting in a head-to-head competition between p and q , which the latter will always
 203 dominate due to lack of infection opportunities which would be granted by a large plasmid free f
 204 population.

205



206

207 **Figure 1.** Phase portraits describing the fate of compensatory mutations. (A) Chromosomal
 208 CMs. (B) Plasmid CMs. Axes describe relative conjugation rates without (x) and with (y) the
 209 corresponding CM, with the black line indicating no difference. Where $\gamma_{CM} > \gamma_P$ (i.e. both

210 growth rate and conjugation rate are increased by the CM, indicated in grey) the wild-type
211 plasmid is always lost with the system reverting to a two-member basic model.

212 //

213

214 Although four-equation models describing a direct competition between chrCM and plaCM
215 cannot be solved analytically, some insight can be gained by comparing equations 3 and 6.
216 Specifically, we can see that as the abundance of plasmid-free recipients decreases, the γ_{Qf}
217 component that positively affects the success of plaCM correspondingly decreases, such that
218 the relative success of plaCM and chrCM is increasingly determined by the difference between
219 β_c and β_q , i.e. the relative strengths of amelioration of the two CMs.

220

221 Overall, then, our models identify a broader range of parameter space in which plaCM is likely
222 to succeed, relative to chrCM. However, we also predict that trade-offs between compensatory
223 mutations and plasmid conjugation can have complex effects on the overall success of a CM,
224 particularly in communities that contain a mixture of uncompensated plasmid-carrying and
225 plasmid-free competitors. Selection reduces the complexity of the dynamics in both cases by
226 removing potential recipients from the system, thus reducing the contribution of plasmid
227 transmission to the dynamics, and increasing the dependency of the outcome on the relative
228 strength of the CM.

229

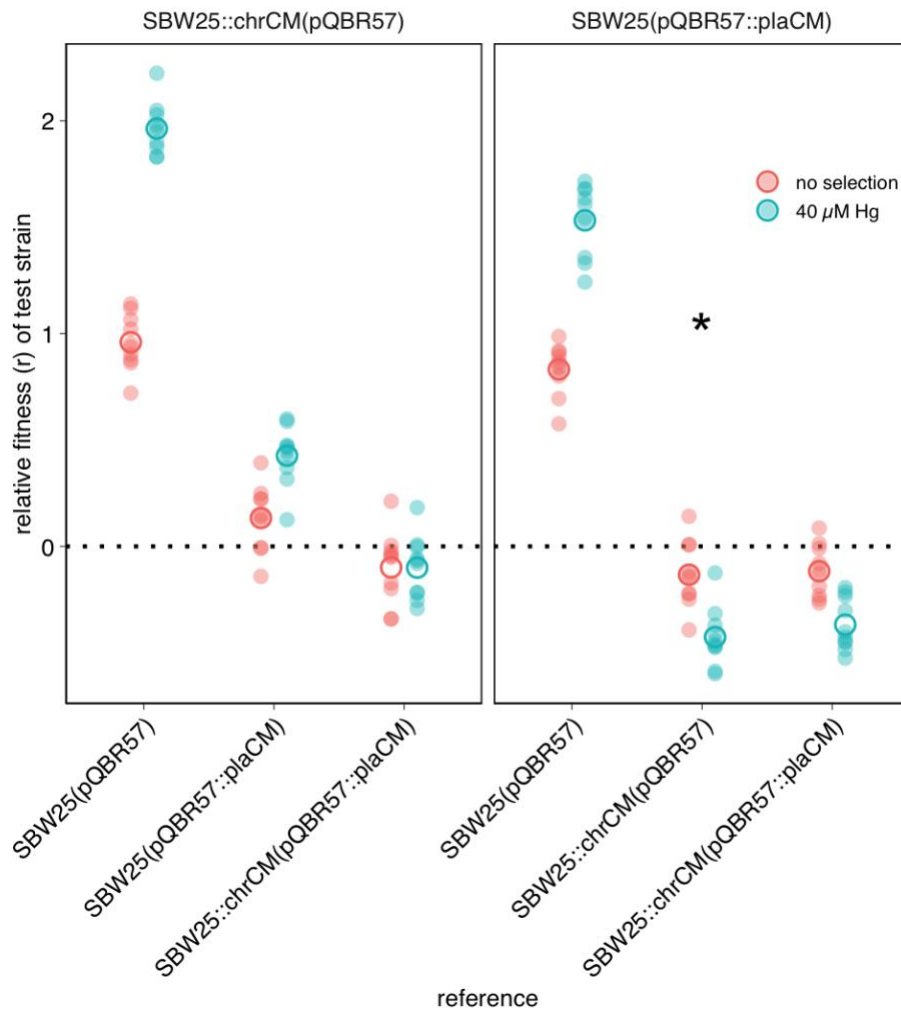
230 ***Knock-outs of putative 'cost' genes recapitulate compensatory mutations***

231 To experimentally investigate the dynamics of plaCM *versus* chrCM, we established an
232 experimental system in which fluorescently-labelled strains were engineered with plaCM or
233 chrCM, enabling enumeration by flow cytometry. To test that our newly-engineered strains
234 exhibited the fitness effects by flow cytometry that we have previously observed by CFU plating,
235 we first performed 24-hour competition experiments. As expected, each CM ameliorated the
236 fitness cost of plasmid carriage (Fig. 2, linear model [LM] one-sided posthoc comparison against
237 0: plaCM $t_9 = 22.1$, $p < 1e-7$; chrCM $t_9 = 23.5$, $p < 1e-7$). In addition, our head-to-head
238 experimental design revealed that chrCM was marginally fitter than plaCM (coefficient = 0.13, t_9
239 = 2.75, $p = 0.045$) and there was no detected fitness benefit of combining both CMs in the same
240 cell (coefficient comparing single vs. double-compensation = -0.1, $t_9 = -1.86$, $p = 0.19$).

241 Interestingly, the benefits of CMs relative to non-compensated plasmid-carrying strains were
242 enhanced in the presence of mercury, and more strongly so for chrCM than for plaCM (chrCM
243 difference in coefficients = 1.0, plaCM difference in coefficients = 0.7), suggesting that the costly

244 cellular disruption caused by pQBR57 is further exacerbated by exposure to mercury (Carrilero
245 et al., 2021). These results cause us to expect acceleration of CM invasion under mercury
246 selection.

247



248

249 **Figure 2.** Engineered plaCM and chrCM variants both ameliorate plasmid fitness costs, though
250 chrCM is more effective. Panels indicate test strains. Unfilled circles indicate mean across 10
251 replicates, each of which is indicated by a semi-transparent filled circle. The asterisk indicates
252 data in the right panel which is also presented in the left panel.

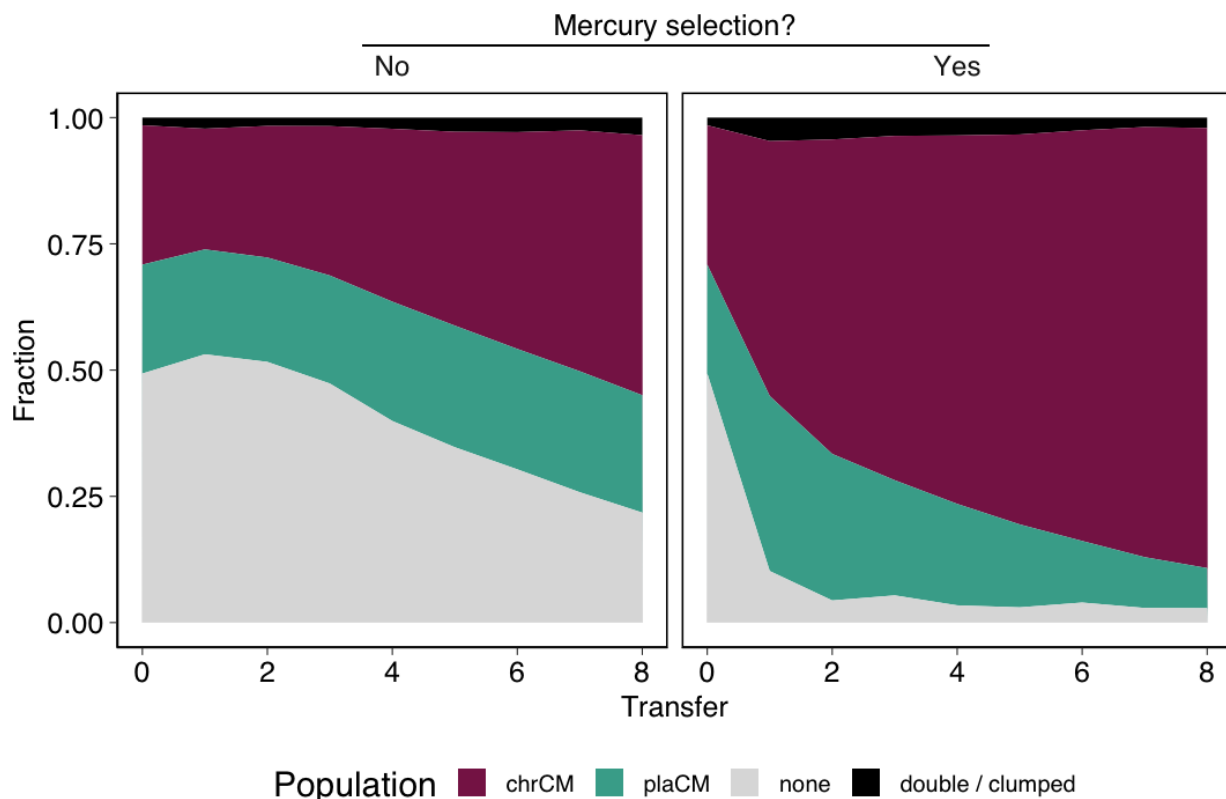
253 //

254

255 ***Chromosomal CM outcompetes plasmid-borne CM across various ecological conditions***

256 To test our predictions, we used our validated strains to test the relative success of chrCM
257 versus plaCM under varying ecological conditions. First, we varied the strength of selection for

258 the plasmid-encoded mercury resistance trait. Informed by our models, we predicted that
259 selection would increase the success of chrCM relative to plaCM. This is because selection
260 would remove plasmid-free recipients from the system, and as plasmids prevent superinfection
261 by similar plasmids through surface exclusion and/or entry exclusion, plaCM would gain no
262 benefit from its ability to transfer by conjugation. For these experiments, our strains were
263 labelled to track the relative success of each mode of compensation, and so the label was
264 inserted into the replicon encoding the compensatory mutation i.e. the SBW25 Δ PFLU4242
265 chromosome for chrCM, and pQBR57 Δ PQBR57_0059 for plaCM. SBW25::chrCM carrying wild-
266 type pQBR57 was competed against pQBR57::plaCM in a wild-type chromosomal background
267 in populations initially containing wild-type plasmid-free recipients at 50% frequency (1:1:2
268 chrCM:plaCM:recipients), and populations were transferred for 8 transfers (~50 generations).
269 Consistent with our predictions, mercury selection indeed favoured chrCM (Fig. 3, Generalised
270 Linear Mixed Effects Model [GLMM] interaction effect of selection:transfer $\chi^2 = 102.9$, $p < 1e-7$,
271 Fig. 3). However, chrCM was also fitter than plaCM without selection (coefficient for transfer = -
272 0.32, $z = -15.7$, $p < 2e-16$), suggesting that any benefits from the ability of the plaCM to transfer
273 into the recipient pool were outweighed by the reduced amelioration provided by plaCM relative
274 to chrCM (Fig. 3).



275

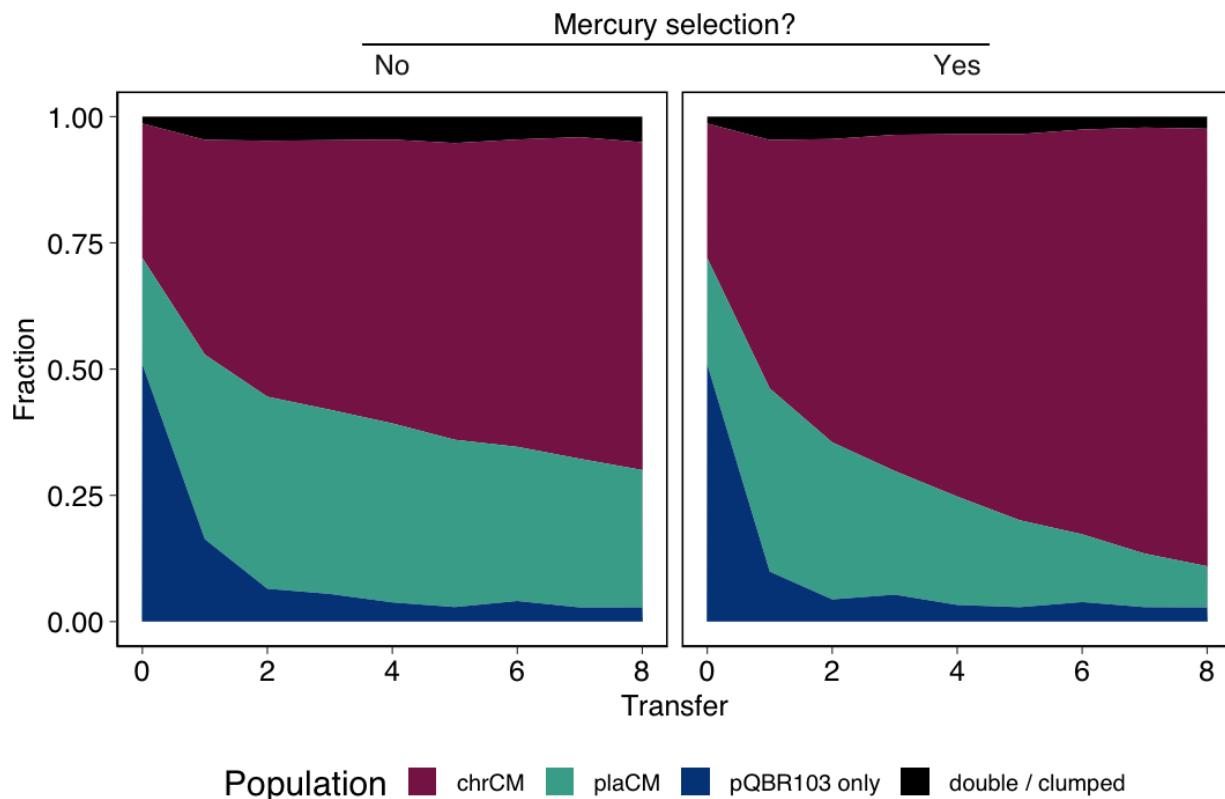
276 **Figure 3.** Chromosomal compensatory mutations outperform plasmid-borne compensatory
277 mutations, particularly under positive selection. Subpanels indicate the presence of mercury
278 selection (No/Yes). Mean of 20 replicates/treatment (10 per marker orientation). Individual
279 replicate plots are shown in Figure S1.

280 //

281

282 In parallel, we investigated whether the benefits of chrCM could be increased in microbial
283 communities hosting multiple costly plasmids. Our previous worked showed that pQBR57 and
284 pQBR103 could be harboured in the same cell. We also showed pQBR103 could be
285 compensated by the chrCM, Δ PFLU4242, both by itself and together with pQBR57, whereas
286 evidence suggested that plaCM exacerbated the cost of pQBR103 (Carrilero et al., 2021; Hall et
287 al., 2021). We therefore predicted that chrCM would be favoured over plaCM both with and
288 without selection in pQBR103-harboring communities, since chrCM would ameliorate both
289 plasmids. Indeed, in communities harbouring pQBR103, chrCM again outcompeted plaCM (Fig.
290 4, GLMM coefficient for transfer = -0.30, $z = -14.5$, $p < 2e-16$, Fig 4), but there was no
291 detectable additional effect of pQBR103 on the relative success of chrCM *versus* plaCM.

292



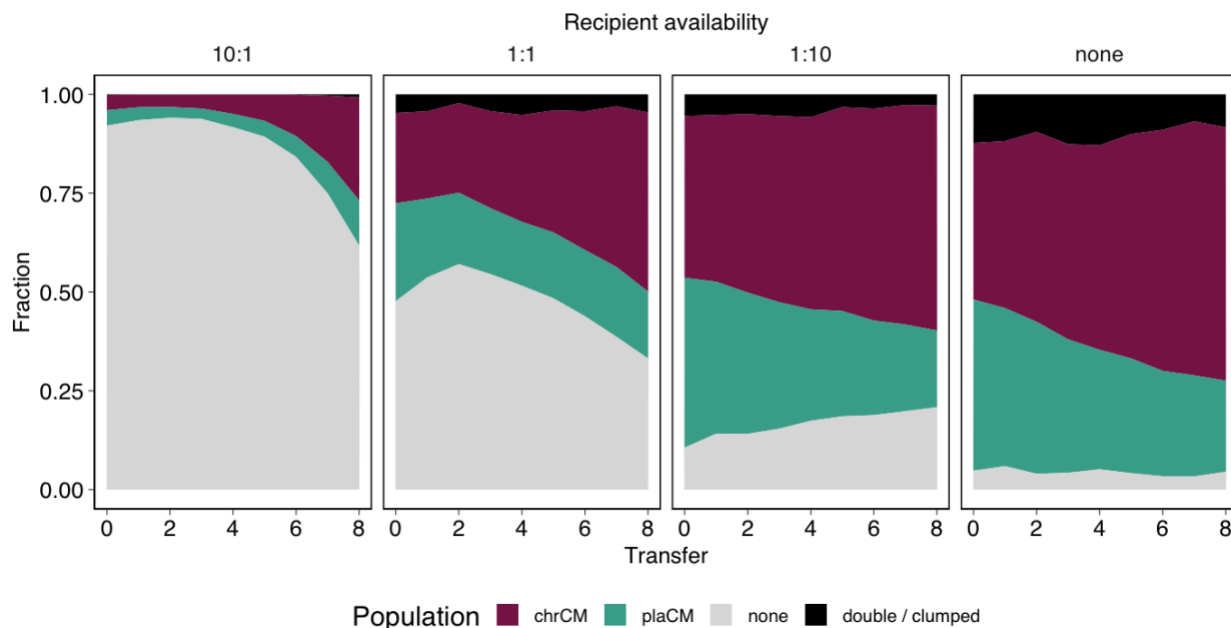
293

294 **Figure 4.** Chromosomal compensatory mutations were not additionally favoured in
295 environments with another costly plasmid. Subpanels indicate the presence of mercury
296 selection (No/Yes). Mean of 20 replicates/treatment (10 per marker orientation). Individual
297 replicate plots are shown in Figure S2.

298 //

299

300 We reasoned that increasing the pool of potential recipients may tip the balance towards plaCM,
301 since conjugation (and thus transmission of the CM) could then play a bigger role in the
302 population dynamics. We again established populations beginning with equal proportions of
303 plaCM and chrCM but varied the proportions of recipients: (i) 10-fold excess of plasmid-free; (ii)
304 equal abundance of plasmid-free; (iii) 10% plasmid-free; (iv) without added plasmid-free.
305 Populations were propagated without selection. Contrary to expectations, plaCM performed
306 relatively poorly against chrCM across all frequencies of plasmid-free recipients (Fig. 5, GLMM
307 transfer:ratio interaction $\chi^2 = 5.00$, $p = 0.17$; main effect of transfer $\chi^2 = 88.6$, $p < 1e-7$;
308 coefficient for transfer = -0.35, $z = -30.8$, $p < 2e-16$), suggesting that the potential benefits of CM
309 transmission could not be manifested by the plaCM.



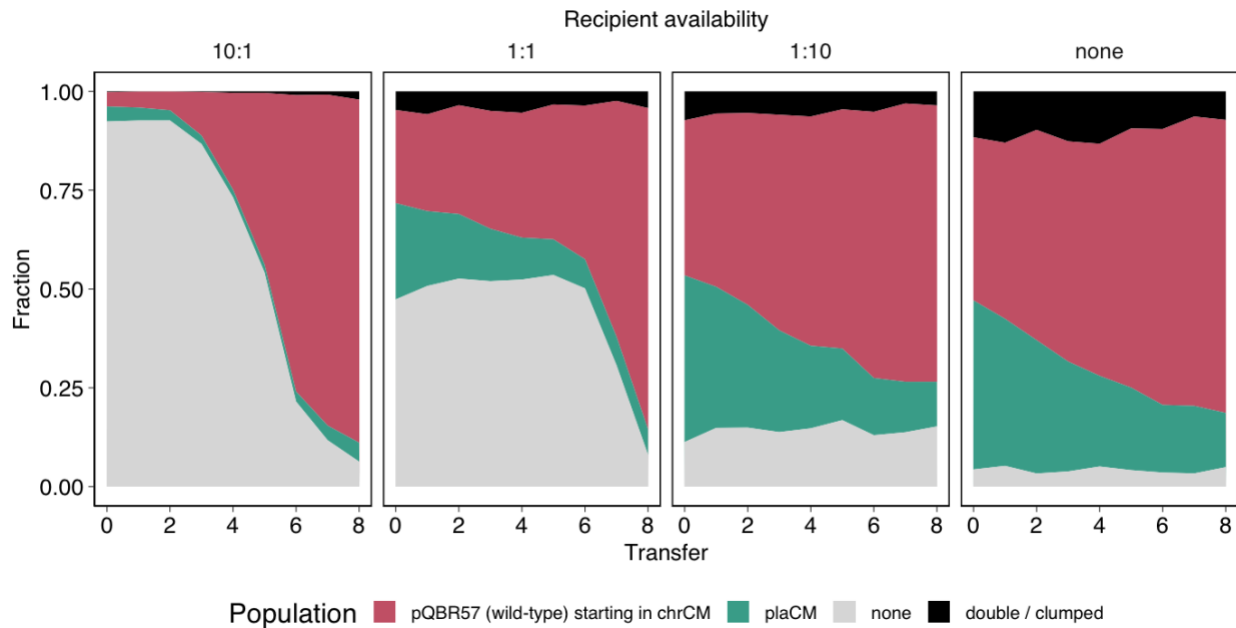
310

311 **Figure 5.** ChrCM was more successful than plaCM regardless of recipient availability. Sub-
312 panels indicate, from left to right, the starting fraction of wild-type/plasmid-free cells relative to a
313 50:50 mix of chromosomal CM (with wild-type plasmid) and plasmid CM in wild-type cells. Plots
314 indicate the mean of 6 independent experiments; replicate-level plots are provided in Figure S3.

315 //

316
317
318
319
320
321
322
323
324
325
326
327
328
329
330
331
332
333
334
335
336
337
338
339
340
341
342

Our model predicted that transmission of wild-type plasmids from chrCM cells could play an important role in the success of chrCM. Furthermore, the theoretical advantage gained by plaCM through horizontal transfer may be reduced when in competition against plasmids carried by cells with chrCM, because wild-type plasmid transfer from chrCM could remove potential recipients for plaCM. However, our initial experiments used fluorescent labels to track the fates of the different compensatory alleles, i.e. the chromosomes of chrCM (SBW25::chrCM), and the plasmids of plaCM (pQBR57::plaCM), rather than the plasmids which began in each background. To understand how the plasmids themselves were affected by the different CMs, we established a complementary experiment to that in Fig. 5, except, rather than tracking chrCM, we tracked the wild-type pQBR57 that began in the chrCM background (Fig. 6). Compared with pQBR57::plaCM, uncompensated pQBR57 from chrCM was significantly more successful, with a considerable proportion of the plasmids at the end of the experiment being uncompensated plasmids that began in the chrCM population, and patterns of invasion depending on the abundance of potential recipients (GLMM third-order polynomial transfer:ratio interaction $\chi^2 = 287.4$, $p < 1e-7$). Notably, comparison with the experiments in Fig. 3 (which were performed in parallel) revealed that invasion of the plasmid from chrCM pre-empted the invasion of chrCM, indicating that plasmid transmission likely contributed to the overall success of chrCM. Essentially, as plasmid-free competitors are removed from the system by infection with the wild-type uncompensated plasmid, the space is filled by competition between CMs, which favours the more effective mechanism of compensation, chrCM. Indeed, when plasmid-free recipients were initially rare, the dynamics essentially come down to a competition between the compensatory mutations, with the most effective mechanism, chrCM, becoming dominant. The experimental results were therefore consistent with our model prediction that transmission of costly plasmids, and the consequent removal of plasmid-free recipients, facilitates the success of chrCM.



343

344

345

346

347

348

349

350

351

352

353

354

355

356

357

358

359

360

361

362

363

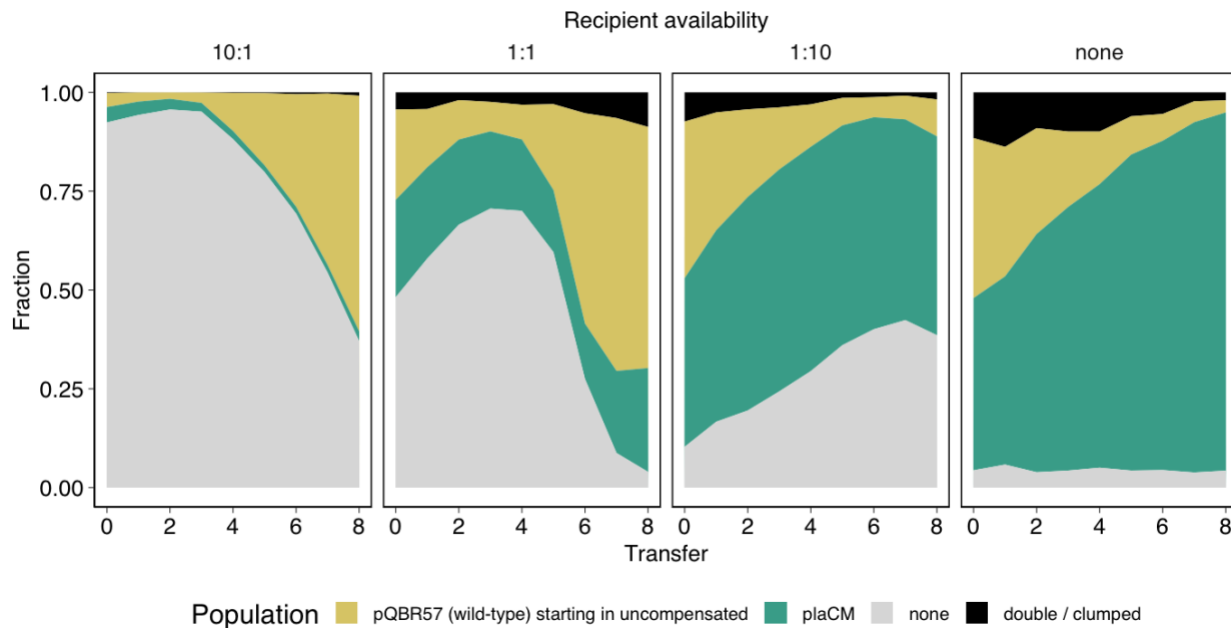
364

Figure 6. Plasmids carried by chrCM cells were more successful than plaCM plasmids regardless of recipient availability. Plots are arranged as Fig. 5. Plots indicate the mean of 6 independent experiments; replicate-level plots are provided in Figure S4.

//

The relative inability of plaCM to invade the recipient population, when compared with wild-type pQBR57 from chrCM cells, suggested that either plaCM exerted a negative pleiotropic effect on the ability of pQBR57 to invade a recipient population, or, conversely, that chrCM enhanced the ability of wild-type pQBR57 to invade. To distinguish between these possibilities, we conducted a similar experiment to Fig. 6, but here, plaCM was competed against pQBR57 harboured by an uncompensated competitor. As with Fig. 6, fluorescent labels were designed to track the relative success of the two plasmids. Unexpectedly, plaCM was only able to outcompete wild-type pQBR57 in the situation where plasmid-free recipients started at low frequency, i.e. effectively a head-to-head competition between compensated and uncompensated plasmid-bearers. We detected a significant effect of plasmid-free recipient ratio on the competition dynamics (GLMM fourth-order polynomial transfer:ratio interaction $\chi^2 = 414.4$, $p < 1e-7$). Specifically, under conditions where recipients were more numerous, wild-type pQBR57 outcompeted the plaCM despite higher fitness costs (Fig. 2), an observation that suggests that plaCM inhibits plasmid transmission (or establishment in transconjugants) relative to the wild-type. Overall, plaCM did not appear to gain a substantive fitness benefit from horizontal transmission, only reaching

365 dominance under conditions that prioritise vertical replication and only in populations without
366 chrCMs.
367



368
369 **Figure 7.** Plasmid-free, uncompensated, and plaCM-compensated plasmids undergo ‘rock-
370 paper-scissors’ cyclical dynamics. Plots are arranged as Fig. 5. Plots indicate the mean of 6
371 independent experiments; replicate-level plots are provided in Figure S5.

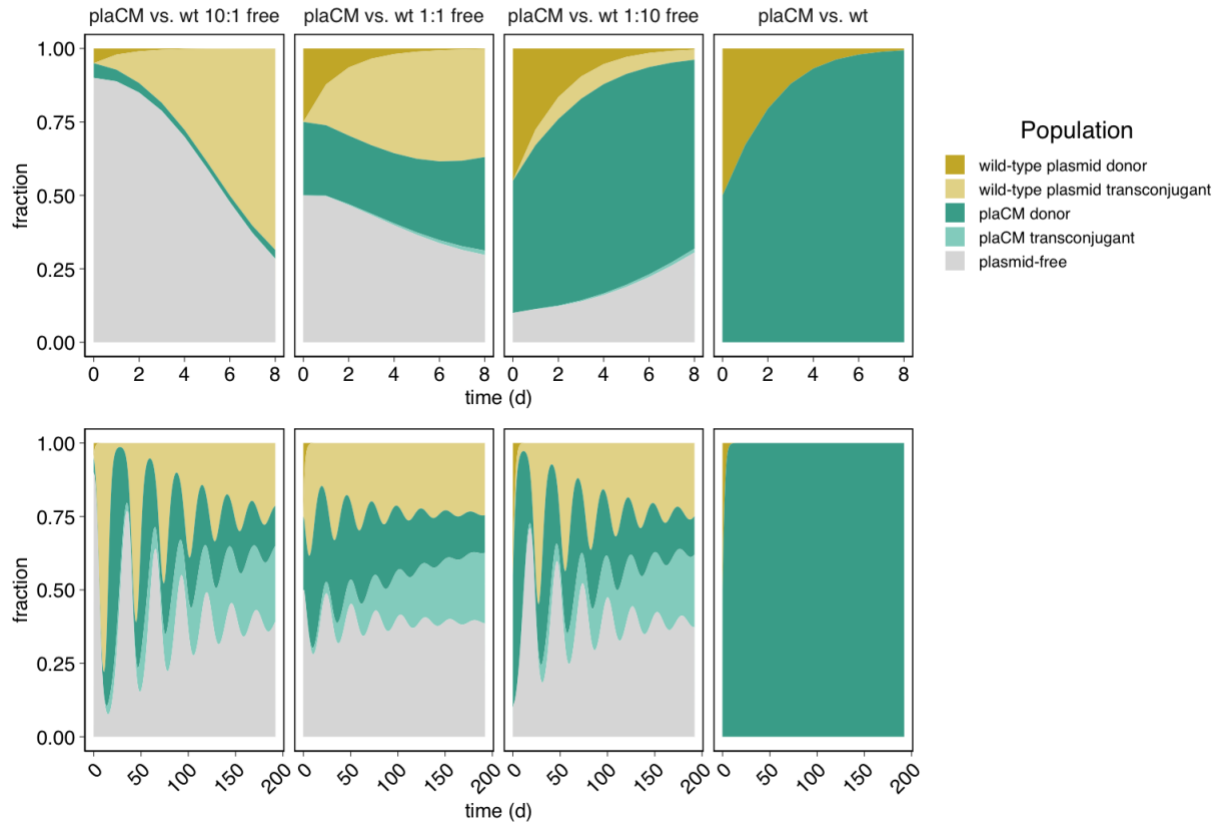
372 //

373

374

375 Our analytical models for plaCM predicted cyclical RPS-like dynamics for some combinations of
376 parameters (Fig 1B orange region). The experimental results in Fig. 7 were consistent with this
377 prediction. Specifically, plasmid-free populations were invaded by the wild-type plasmid (left
378 panel, and mid-left panel after transfer 4), the wild-type plasmid was outcompeted by plaCM
379 (right panel, mid-right panel, and mid-left panel before transfer 4), and plaCM was outcompeted
380 by plasmid-free (mid-right panel). To explore the dynamics in further detail we experimentally
381 determined key parameters in our system (Table S1) and compared these with the analytical
382 model (Fig. 1). With our system, and with experimentally-measured parameter values, the
383 uncompensated plasmid exceeds the threshold for plasmid invasion and domination, which is
384 indeed what we have described previously (Stevenson et al., 2017). Both chrCM and plaCM
385 likewise exceed the threshold for domination by 18- and 10-fold respectively, indicating that,
386 with sufficient reduction in γ_Q relative to γ_P , the plaCM system might exist in the (f^*, p^*, q^*) region

387 of parameter space. Numerical simulations based on equations 1–6 and Supplementary
388 Equations 1, and parameterised with biologically-plausible values, resulted in dynamics
389 resembling observed experimental results, provided plaCM decreased conjugation rate
390 sufficiently (10–100×, Fig. 8). An interactive (Shiny) app enabling readers to explore these
391 patterns is provided at (jpih.shinyapps.io/COMPMOD_shiny).
392



393
394 **Figure 8.** ODE-based model simulations resemble experimental results. Numerical simulations
395 of a batch-transfer model using the following parameters: $\alpha = 0.6 \text{ h}^{-1}$, SBW25(pQBR57) relative
396 fitness = 0.82, SBW25(pQBR57::plaCM) relative fitness = 0.95, $K = 5.7 \times 10^9 \text{ ml}^{-1}$,
397 uncompensated conjugation rate = $9.9 \times 10^{-12} \text{ ml} \cdot \text{cells}^{-1} \cdot \text{h}^{-1}$, plaCM conjugation rate = 1.3×10^{-13}
398 $\text{ml}/\text{cells}/\text{h}$; $\gamma_P \sim 75 \times \gamma_Q$. Top panels indicate dynamics over 8 transfers, bottom panels over 192
399 transfers. Details on parameterisation are provided in Supplementary Table 1. An interactive
400 version of this figure is provided at jpih.shinyapps.io/COMPMOD_shiny.

401 //
402

403 Together, our experimental and modelling results suggested that plaCM has a negative
404 pleiotropic effect on conjugative transmissibility. Previous attempts to measure the intraspecific
405 conjugation rates of pQBR57 with and without chrCM/plaCM did not detect any significant
406 differences from the wild-type pQBR57 (Hall et al., 2021). However, these experiments were
407 conducted over a relatively long time window (24 hr), which could allow fitness differences
408 between transconjugants, donors, and recipients to mask differences in transfer rate (Huisman
409 et al., 2022; Kosterlitz et al., 2022). We therefore re-measured conjugation rate using the
410 Approximate Extended Simonsen approach (Huisman et al., 2022) — an extension to the
411 popular ‘Simonsen’s gamma’ (Simonsen et al., 1990) that accommodates the potential for
412 variation in growth rate. Unexpectedly, we did not detect any significant difference between the
413 wild-type and plaCM variants of pQBR57, and certainly not the order-of-magnitude difference
414 predicted by the model (Figure S6; $t_{9,86} = 0.75$, $p = 0.94$, TOST equivalence test with \log_{10} -
415 transformed bounds ± 0.5 , $p = 0.02$). We therefore hypothesise that the differences in pQBR57
416 transmissibility between wild-type and plaCM variants observed in Fig. 7 emerge from yet-to-be-
417 determined processes following plasmid establishment in recipient cells.

418

419 **Discussion**

420 Plasmid fitness cost amelioration is an important process driving the maintenance, distribution,
421 and dissemination of plasmids and their associated traits. Where plasmid fitness costs are
422 generated from an interaction between the plasmid and resident chromosomal genes, mutations
423 affecting either of these partners can enable plasmid survival. Previous experimental evolution
424 studies on CMs have generally implicated chromosomal loci rather than plasmid loci as the
425 principal targets, a finding which has been taken to reflect mutational supply, availability, and/or
426 the poor ability of oftentimes recessive compensatory mutations to penetrate when appearing
427 on a multi-copy plasmid (Mei et al., 2019; Stalder et al., 2017). But although more difficult to
428 access, plaCMs, once achieved, ought to be more successful than chrCMs under a range of
429 ecological conditions owing to the simple fact that plaCM is propagated when the plasmid
430 transfers into recipients (Zwanzig et al., 2019). The relatively high transfer rate of pQBR57
431 ought to have further accentuated this benefit (Hall et al., 2015), particularly under
432 environmental conditions with high recipient availability. In contrast to these expectations, our
433 analyses and experiments showed that plaCM was not successful under most tested conditions,
434 losing out to chrCM, wild-type plasmids harboured by chrCM-containing cells, and even, where
435 opportunities for HGT were plentiful, wild-type plasmids from cells lacking CMs.

436

437 There are several processes that could explain the relative failure of plaCM. First, our analyses
438 of extensions to a simple plasmid population dynamics model reveal that for transmissible
439 plasmids, chrCMs provide a hidden benefit besides directly reducing the fitness cost of plasmid
440 carriage to their bearers: conjugation from chrCM-containing cells transforms plasmid-free
441 competitors into plasmid-carriers suffering the full burden of uncompensated plasmid carriage,
442 indirectly enhancing the relative fitness of chrCM. Previous numerical simulations have likewise
443 demonstrated the possibility for ‘weaponisation’ of conjugative elements through compensatory
444 mutation, and such a dynamic provides a further explanation for the persistence of non-
445 beneficial plasmids in communities (Domingues et al., 2022; Rebelo et al., 2023b, 2023a). Our
446 analyses generalise these findings and demonstrate that a high degree of amelioration and low
447 impact on transmissibility will enhance chrCM invasion, particularly if the local chrCM frequency
448 is sufficiently high, a condition that is more likely to be met in spatially-structured habitats and/or
449 where chrCM confers pleiotropic environmentally-adaptive benefits (Kloos et al., 2021; Loftie-
450 Eaton et al., 2017; Rebelo et al., 2023a). Thus, the marginal benefits of conjugative
451 transmissibility for plaCM in competition with chrCM are reduced.

452

453 Second, the benefits to plaCM of conjugative transmission wane as the plasmid-free recipient
454 pool is diminished, from either (i) selection against plasmid-free recipients, or (ii) recipient
455 acquisition of plasmids that can bar the incoming plaCM by incompatibility or exclusion. We
456 observed both dynamics in our experiments. The effects of the latter mechanism are even more
457 pronounced if there is a mechanistic trade-off between compensating plasmid fitness costs and
458 the ability of the plasmid to transfer or establish in recipients, such as our results suggest, since
459 a more transmissible (but more costly) plasmid can sweep through the recipient population,
460 blocking access for the plaCM. Once the plasmid-free population is diminished, the dynamics of
461 the system are driven by the relative growth rates of the different subpopulations, which in turn
462 are determined by the degree of amelioration provided by chrCM and plaCM. In our system,
463 SBW25::chrCM(pQBR57) outgrows SBW25(pQBR57::plaCM) in direct competition, because
464 plaCM is not as efficient as chrCM at compensating the fitness cost of pQBR57. This
465 discrepancy is likely due to the molecular mechanisms that underpin the principal fitness costs
466 of pQBR57 and their resolution by compensatory mutation. PFLU4242 is a putative
467 endonuclease, with a DUF262/DUF1524 domain structure resembling that of the GmrSD type
468 IV restriction system (Machnicka et al., 2015), and so we hypothesised that this gene is
469 somehow directly responsible for generating the dsDNA breaks that trigger the SOS response
470 and subsequent toxic gene expression patterns characteristic of uncompensated pQBR57

471 carriage (Hall et al., 2021). Loss-of-function mutations to PFLU4242 (i.e. chrCM) would directly
472 prevent these breaks from occurring. On the other hand, *PQBR57_0059* encodes a lambda
473 repressor-like protein that regulates expression of two other pQBR57-encoded putative DNA-
474 binding proteins, *PQBR57_0054-0055*, and it is upregulation of *PQBR57_0054-0055* which
475 provides the proximal mechanism of plaCM compensation, through a mechanism not yet fully
476 understood. ChrCM therefore likely provides a more direct route than plaCM to resolving the
477 genetic conflict at the heart of pQBR57-SBW25 fitness costs, and thus is mechanistically a more
478 effective CM. Ultimately, it is likely to be the degree to which CMs reduce the cost of plasmid
479 carriage, rather than CM transmissibility, which will primarily determine CM success.

480

481 Unexpectedly, plaCM was a poor competitor against the wild-type uncompensated pQBR57,
482 winning out only in cases where there were few opportunities for conjugation. This experimental
483 observation, coupled with our model parameterisation and numerical simulations, strongly
484 implies that pQBR57::plaCM is not as effective as the wild-type plasmid at transmitting by
485 conjugation and/or establishing in recipients. As measured conjugation rates of wild-type
486 pQBR57 and pQBR57::plaCM have been indistinguishable, even when controlling for the
487 different fitness effects of the two plasmids, these observations imply that differences in
488 transmissibility emerge from processes other than plasmid transfer *per se*. *PQBR57_0055* is a
489 Spo0J/ParB-like protein, homologues of which have been shown to have various, non-specific
490 effects on gene expression, and by upregulating *PQBR57_0054-0055*, plaCM could have
491 various pleiotropic effects in transconjugants. For example, plasmids have been shown to
492 impose transient costs on acquisition, mainly driven by increased in lag time and usually
493 resolved in a matter of hours, alongside the longer lasting fitness costs (Ahmad et al., 2023;
494 Prenskey et al., 2021). Additionally, some plasmids exhibit 'conjugation derepression', whereby,
495 for a short period, transconjugants display an increased onward conjugation rate. The extent
496 and duration of such 'acquisition costs' and conjugation derepression may vary between plaCM
497 and wild-type to disfavour plaCM transmission without having a direct impact on transmission
498 rate. Overall, our experiments comparing pQBR57::plaCM and wild-type pQBR57 are congruent
499 with several other studies demonstrating trade-offs between vertical and horizontal plasmid
500 transmission (Bethke et al., 2023; Dahlberg and Chao, 2003; Dimitriu et al., 2021; Porse et al.,
501 2016; Turner et al., 2014), and further show that imperfect plaCMs that trade-off against
502 transmission can generate long-standing oscillatory dynamics which could sustain diversity in
503 the plasmid population.

504

505 The chrCM in our system ameliorates diverse other mercury resistance plasmids, including
506 pQBR103 and pQBR55 (Hall et al., 2021, 2019), and can ameliorate the costs of co-habiting
507 compatible plasmids (Carrilero et al., 2020). Previous work has likewise shown the generality of
508 chromosomal compensatory mutations in reducing the fitness costs of different plasmids (Loftie-
509 Eaton et al., 2017). Our experiments did not detect a beneficial effect on chrCM vs. plaCM when
510 pQBR103 was introduced, likely because the low conjugation rate of pQBR103, overall benefit
511 of chrCM, and short period of the experiment meant that any selective pressure imposed by
512 pQBR103 acquisition was negligible. Nevertheless, the fact that chrCM was more likely to
513 outcompete plaCM even in a single-plasmid (pQBR57) system indicates that lineages gaining
514 CMs can become pre-disposed to acquiring further plasmids, potentially becoming hubs for
515 horizontal gene transfer, plasmid recombination, and trait dissemination in microbial
516 communities. Efforts to limit HGT, for example to control the spread of antibiotic resistance,
517 should therefore focus on identifying and targeting such ‘keystone’ strains. One possible route
518 would be to use antagonistic parasitic MGEs such as lytic bacteriophage. The target of chrCM in
519 our system appears related to GmrSD, a known genome defence mechanism, and while little
520 was known of the biological function of the *P. aeruginosa* PAO1 chrCM targets identified by San
521 Millan et al. (San Millan et al., 2015) at the time of discovery, gene function prediction tools now
522 associate the accessory helicase PA1372 and partner gene PA1371 with genome defence
523 (‘Helicase + DUF2290 system’) (Payne et al., 2021; Tesson et al., 2022). Likewise, the
524 ‘Xpd/Rad3-like helicase’ and ‘upstream UvrD helicase’ targets of chrCMs identified by Loftie-
525 Eaton et al. (Loftie-Eaton et al., 2017) in *Pseudomonas* sp. H12 refer to predicted components
526 of prokaryotic Argonaute type III and Gabija respectively, while in *Vibrio*, a recently-discovered
527 defence system DdmABC confers a high fitness cost on bearers of large plasmids such that
528 they are removed from a population by purifying selection in a manner that resembles the large
529 fitness cost imposed by PFLU4242 (Jaskólska et al., 2022). The ability of ‘MGE-favourable’
530 organisms to receive and host plasmids thus likely trades off against susceptibility to costly
531 parasitic elements, and exploiting this weakness may be a profitable approach to controlling the
532 maintenance and spread of unwanted mobile genetic elements in various microbiomes.

533

534 Though some aspects — namely the relative degree to which chrCM and plaCM ameliorate
535 plasmids and the extent to which plaCM imposes pleiotropic effects on conjugation rate — may
536 be system specific, the superiority of chromosomal CMs over plasmid-borne CMs in terms of
537 mutational accessibility, indirect effects on plasmid-free competitors (as presented here with a
538 general theoretical mechanism), mechanistic efficacy, and reduced potential for trade-off with

539 horizontal transmission, are likely to generalise to diverse other plasmid-bacterial pairings,
540 including pathogens and multi-drug resistance plasmids. One broader implication is that
541 transmissible plasmids thus have a limited ability to ‘act nice’ by effectively ameliorating their
542 own costs by evolution. Instead, plasmids are under stronger selection to improve their
543 transmissibility and intracellular competitiveness, and it is largely down to resident genes to
544 accommodate these unruly vectors — or remove them.

545

546 **Acknowledgements**

547 This work was supported by the Natural Environment Research Council (NE/R008825/1) to
548 MAB, EH, AJW, SP, JPJH. RCW is supported by a funding from the Biotechnology and
549 Biosciences Research Council to RCW and MAB (BB/T014342/1). JPJH is supported by an
550 MRC Career Development Award (MR/W02666X/1). MJB is supported by the Wellcome Trust
551 Sir Henry Wellcome Fellowship (221663/Z/20/Z).

552

553 **Author contributions**

554 Conceptualization: RCTW, AJW, SP, EH, MAB, JPJH. Data curation: RCTW, JPJH,
555 Investigation: RCTW, AJW, MJB, JPJH. Resources: RCTW, KJM, JPJH. Formal analysis:
556 RCTW, AJW, MJB, JPJH. Funding acquisition: MAB, EH, AJW, SP, JPJH. Visualization: RCTW,
557 AJW, MJB, JPJH. Writing — original draft: RCTW, AJW, MAB, JPJH. Writing — review &
558 editing: RCTW, AJW, MJB, EH, MAB, JPJH.

559

560 **Methods**

561 ***Bacterial strains***

562 Fluorescently-labelled strains of *Pseudomonas fluorescens* SBW25 and *P. fluorescens*
563 SBW25 Δ PFLU4242 (Hall et al., 2019) were generated using the mini-Tn7 system and plasmid
564 pUCT-mini-Tn7T-Gm-eyfp (Choi and Schweizer, 2006) or a derivative in which dTomato was
565 cloned to replace eyfp. The pQBR57 Δ pQBR57_0059 knockout, and fluorescently-labelled
566 variants of megaplasmid pQBR57 (Hall et al., 2015; Lilley et al., 1996) were generated using
567 homologous recombination with plasmid pTS-1 (Campilongo et al., 2017). Briefly, for the
568 knockout, 1 kb flanking regions of pQBR57 were amplified and cloned into the MCS of Xba-
569 KpnI-digested pTS-1 using NEB HiFi assembly. For the fluorescently-labelled plasmids,
570 fragments of pQBR57 and an expression cassette consisting of a Ptac promoter driving a
571 fluorescence protein gene (either eGFP or tdTomato), followed by lambda t0 and rrnB T1
572 terminators were amplified and cloned into the MCS of XhoI/KpnI-digested pTS-1 using NEB

573 HiFi assembly. Constructs were transformed into SBW25(pQBR57) by electroporation (Choi
574 and Schweizer, 2006), and merodiploids selected on KB supplemented with 100 µg/ml
575 tetracycline. Double-crossovers were selected on LB supplemented with 10% w/v sucrose and
576 20 µM HgCl₂, and candidates screened by PCR and tetracycline sensitivity before sending for
577 whole genome sequencing (2x250 bp, >30x coverage, MicrobesNG) to test for second-site
578 mutations. Using breseq (Deatherage and Barrick, 2014), no second-site mutations were
579 detected for the strains used in these experiments. For experiments, each plasmid-containing
580 replicate was established with an independent transconjugant from a genome-sequenced donor
581 strain. Conjugation experiments were performed with non-fluorescent antibiotic-labelled
582 strains described previously (Hall et al., 2021).

583

584 **Competition experiment**

585 To determine the short-term fitness effects of compensation, direct competitions were performed
586 between YFP- *versus* dTomato-labelled strains. Overnight cultures were mixed at 1:1 ratio
587 (test:reference) before inoculation at 1:100 dilution into 6 ml King's B media in a 30 ml glass
588 universal with loose-fitting lid ('microcosm'), with or without mercury (Hg (II), 40 µM) and incubated
589 at 28°C, 180 rpm for 24 hours. Each competition was repeated with 10 biological replicates. Flow
590 cytometry was used to estimate bacterial counts: starting mixtures and endpoint competition
591 cultures were diluted 1:100 into M9 buffer and run on a Beckman Coulter CytoflexS machine at
592 17 µl.min⁻¹ for either 5,000 counts (determined as events with signal in SSC-H channel > 10³) or
593 90 seconds maximum. Between samples, M9 buffer was sampled for 5 seconds to minimise
594 cross-over between samples. Strain counts were determined by gating in the following channels:
595 FITC-H (gate=10^{3.4} for YFP) and PE-H (gate=10^{3.4} for dTomato). Relative fitness was calculated
596 as the difference in Malthusian parameters, $r = \ln\left(\frac{test_{end}}{test_{start}}\right) - \ln\left(\frac{reference_{end}}{reference_{start}}\right)$.

597

598 **Serial passage experiments**

599 For all evolution experiments, bacterial populations were grown in 6 ml KB microcosms at 28°C
600 with agitation at 180 rpm. Serial daily transfers of 1% population into fresh media were performed
601 for 8 days, with daily flow cytometry used to track population dynamics. For flow cytometry,
602 cultures were diluted 1:100 into M9 buffer and incubated with Hoechst 34580 stain (5 µg/ml) for
603 15 minutes in the dark at room temperature to enable detection of unlabelled bacterial strains.
604 Flow cytometry data was sampled for 60 seconds at 17µl.min⁻¹ with minimal gating for size (FSC-
605 H > 10³), and strain counts were determined in post analysis with the following thresholds:

606 Hoechst-stained bacteria (i.e., total bacterial count, PB450-H > 10⁴), YFP only (FITC-H > 10^{3.5}),
607 dTomato only (PE-H > 10^{3.4}), YFP+dTomato clumps (FITC-H > 10^{3.5} and PE-H > 10^{3.4}). Between
608 samples, M9 buffer was sampled for 5 seconds to minimise cross-over between samples. For
609 each fluorescently labelled strain, single-strain populations (3 biological replicates) were serially
610 transferred for the duration of the experiment to ensure maintenance of the fluorescent signal.

611

612 To investigate the benefit of differing modes of compensation under varying selection pressures,
613 we first challenged equal proportions of plaCM (SBW25(pQBR57Δ0059)) against chrCM
614 (SBW25ΔPFLU4242(pQBR57)) in the presence of either a plasmid-free wild-type host (SBW25)
615 or a wild-type host bearing a more costly conjugative plasmid (SBW25(pQBR103)). In all
616 populations, the wild-type host started at ~50% frequency and carried a gentamicin resistance
617 marker (Gm^R). In a fully factorial design, each population was grown in either in the presence or
618 absence of mercury (Hg (II), 40 μM). Fluorescent markers (YFP or dTomato) associated with each
619 mode of compensation allowed tracking of population dynamics in the presence of a non-
620 fluorescent wild-type strain, with 10 biological replicates per marker orientation.

621

622 The impact of host availability on the benefit of plaCM was investigated in a separate evolution
623 experiment, by challenging GFP-labelled plaCM (SBW25(pQBR57Δ0059::GFP)) against different
624 host:plasmid backgrounds in the presence of varying ratios of plasmid-free wild-type hosts
625 (SBW25::Gm^R), including 10x excess, equal proportions, 10x fewer and no available hosts. At
626 each level of host availability, plaCM was competed against chrCM with a chromosomally-
627 encoded fluorescent label (SBW25Δ4242::dTomato(pQBR57)), chrCM with a plasmid-encoded
628 fluorescent label (SBW25Δ4242(pQBR57::tdTomato)) or a wild-type plasmid bearer
629 (SBW25(pQBR57::tdTomato)). For each treatment, 6 biological replicates were performed. Raw
630 data from flow cytometry experiments are provided at <https://doi.org/10.5285/51046841-deaa-422f-a303-2c0759f014b4>.

631

632 **Conjugation rates**

634 Streptomycin-resistant *lacZ*-carrying donors (either SBW25(pQBR57) or
635 SBW25(pQBR57ΔpQBR57_0059)), Gm^R recipients (SBW25), and Gm^R transconjugants (either
636 SBW25(pQBR57) or SBW25(pQBR57ΔpQBR57_0059)), cultured overnight in 150 μl KB broth
637 in an untreated CytoOne 96-well microtitre plate at 28°C, were subcultured 1:30 into 150 μl
638 fresh media and placed in a Tecan Nano plate reader for incubation at 28°C with shaking. When
639 exponential phase was reached (assessed by examination of growth curves; OD₆₀₀ ~ 0.4)

640 cultures were again diluted 30-fold into KB. Mixed cultures containing donors and recipients, or
641 single-strain donor, recipient, or transconjugant cultures were sampled and cultured in the plate
642 reader and spread on KB agar plates supplemented with 50 µg/ml X-gal for enumeration. After
643 approx. 4 hours growth, cultures were again sampled and spread on KB agar plates, some of
644 which were supplemented with antibiotics (250 µg/ml streptomycin or 30 µg/ml gentamicin) and
645 20 µM mercury to enumerate transconjugants. Conjugation rates were calculated with the
646 Approximate Extended Simonsen Method (Huisman et al., 2022).

647

648 **Statistics**

649 Relative fitness was analysed using linear models, with post-hoc pairwise comparisons
650 performed using the package emmeans (Lenth, 2023). Dynamics were analysed with
651 Generalized Linear Mixed Effects Models (GLMM) using the R package glmmTMB (Brooks et
652 al., 2017), with a beta-binomial response distribution, a logit link function, and the counts of
653 each competitor as the response variables. Preliminary analyses identified overdispersion in the
654 data, justifying the use of a beta-binomial rather than a binomial response distribution (Harrison,
655 2015). Non-independence of measurements arising from repeated sampling of populations was
656 accommodated with random effects of ‘population’ on intercept and slope, except for the
657 experiment presented in Fig. 7 which included only the random effect on intercept due to
658 extremely low variance and high correlation between random effects preventing model
659 convergence. For experiments presented in Figs. 6 and 7, polynomial terms were added to
660 accommodate potentially non-monotonic relationships between competitors over time.
661 Significance of fixed effects were determined by comparison of nested models using likelihood
662 ratio tests. Conjugation rate data were analysed by t-test and two one-sided tests using the
663 package TOSTER (Lakens et al., 2018). Data and analysis scripts are provided at
664 https://github.com/jpjh/COMPMUT_dynamics.

665

666

667 **References**

668

669 Ahmad M, Prensky H, Balestrieri J, EINaggar S, Gomez-Simmonds A, Uhlemann A-C, Traxler
670 B, Singh A, Lopatkin AJ. 2023. Tradeoff between lag time and growth rate drives the
671 plasmid acquisition cost. *Nat Commun* **14**:1–12.

- 672 Bailey MJ, Lilley AK, Thompson IP, Rainey PB, Ellis RJ. 1995. Site directed chromosomal
673 marking of a fluorescent pseudomonad isolated from the phytosphere of sugar beet;
674 stability and potential for marker gene transfer. *Mol Ecol* **4**:755–763.
- 675 Benz F, Hall AR. 2022. Host-specific plasmid evolution explains the variable spread of clinical
676 antibiotic-resistance plasmids. *bioRxiv*. doi:10.1101/2022.07.06.498992
- 677 Bethke JH, Ma HR, Tsoi R, Cheng L, Xiao M, You L. 2023. Vertical and horizontal gene transfer
678 tradeoffs direct plasmid fitness. *Mol Syst Biol* **19**. doi:10.15252/msb.202211300
- 679 Bottery MJ, Wood AJ, Brockhurst MA. 2017. Adaptive modulation of antibiotic resistance
680 through intragenomic coevolution. *Nat Ecol Evol* **1**:1364–1369.
- 681 Brockhurst MA, Harrison E. 2022. Ecological and evolutionary solutions to the plasmid paradox.
682 *Trends Microbiol* **30**:534–543.
- 683 Brooks M, Kristensen K, Benthem K van, Magnusson A, Berg C, Nielsen A, Skaug H, Mächler
684 M, Bolker B. 2017. GlimmTMB balances speed and flexibility among packages for zero-
685 inflated generalized linear mixed modeling. *R J* **9**:378.
- 686 Campilongo R, Fung RKY, Little RH, Grenga L, Trampari E, Pepe S, Chandra G, Stevenson
687 CEM, Roncarati D, Malone JG. 2017. One ligand, two regulators and three binding sites:
688 How KDPG controls primary carbon metabolism in *Pseudomonas*. *PLoS Genet*
689 **13**:e1006839.
- 690 Carrilero L, Kottara A, Guymer D, Harrison E, Hall JPJ, Brockhurst MA. 2021. Positive Selection
691 Inhibits Plasmid Coexistence in Bacterial Genomes. *MBio* **12**. doi:10.1128/mBio.00558-
692 21
- 693 Carrilero L, Kottara A, Guymer D, Harrison E, Hall JPJ, Brockhurst MA. 2020. Positive selection
694 inhibits plasmid coexistence in bacterial genomes. *Cold Spring Harbor Laboratory*.
695 doi:10.1101/2020.09.29.318741
- 696 Choi K-H, Schweizer HP. 2006. mini-Tn7 insertion in bacteria with single attTn7 sites: example
697 *Pseudomonas aeruginosa*. *Nat Protoc* **1**:153–161.
- 698 Dahlberg C, Chao L. 2003. Amelioration of the cost of conjugative plasmid carriage in
699 *Escherichia coli* K12. *Genetics* **165**:1641–1649.
- 700 De Gelder L, Ponciano JM, Joyce P, Top EM. 2007. Stability of a promiscuous plasmid in
701 different hosts: no guarantee for a long-term relationship. *Microbiology* **153**:452–463.
- 702 Deatherage DE, Barrick JE. 2014. Identification of mutations in laboratory-evolved microbes
703 from next-generation sequencing data using breseq. *Methods Mol Biol* **1151**:165–188.

- 704 Dimitriu T, Matthews AC, Buckling A. 2021. Increased copy number couples the evolution of
705 plasmid horizontal transmission and plasmid-encoded antibiotic resistance. *Proc Natl*
706 *Acad Sci U S A* **118**. doi:10.1073/pnas.2107818118
- 707 Domingues CPF, Rebelo JS, Monteiro F, Nogueira T, Dionisio F. 2022. Harmful behaviour
708 through plasmid transfer: a successful evolutionary strategy of bacteria harbouring
709 conjugative plasmids. *Philos Trans R Soc Lond B Biol Sci* **377**:20200473.
- 710 Finks SS, Martiny JBH. 2023. Plasmid-Encoded Traits Vary across Environments. *MBio*
711 **14**:e0319122.
- 712 Hall JPJ, Harrison E, Lilley AK, Paterson S, Spiers AJ, Brockhurst MA. 2015. Environmentally
713 co-occurring mercury resistance plasmids are genetically and phenotypically diverse and
714 confer variable context-dependent fitness effects. *Environ Microbiol* **17**:5008–5022.
- 715 Hall JPJ, Wright RCT, Guymer D, Harrison E, Brockhurst MA. 2019. Extremely fast amelioration
716 of plasmid fitness costs by multiple functionally diverse pathways. *Microbiology*.
717 doi:10.1099/mic.0.000862
- 718 Hall JPJ, Wright RCT, Harrison E, Muddiman KJ, Jamie Wood A, Paterson S, Brockhurst MA.
719 2021. Plasmid fitness costs are caused by specific genetic conflicts enabling resolution
720 by compensatory mutation. *PLoS Biol* **19**:e3001225.
- 721 Harrison E, Guymer D, Spiers AJ, Paterson S, Brockhurst MA. 2015. Parallel compensatory
722 evolution stabilizes plasmids across the parasitism-mutualism continuum. *Curr Biol*
723 **25**:2034–2039.
- 724 Harrison XA. 2015. A comparison of observation-level random effect and Beta-Binomial models
725 for modelling overdispersion in Binomial data in ecology & evolution. *PeerJ* **3**:e1114.
- 726 Huisman JS, Benz F, Duxbury SJN, de Visser JAGM, Hall AR, Fischer EAJ, Bonhoeffer S.
727 2022. Estimating plasmid conjugation rates: A new computational tool and a critical
728 comparison of methods. *Plasmid* **121**:102627.
- 729 Jaskólska M, Adams DW, Blokesch M. 2022. Two defence systems eliminate plasmids from
730 seventh pandemic *Vibrio cholerae*. *Nature* **604**:323–329.
- 731 Jordt H, Stalder T, Kosterlitz O, Ponciano JM, Top EM, Kerr B. 2020. Coevolution of host–
732 plasmid pairs facilitates the emergence of novel multidrug resistance. *Nature Ecology &*
733 *Evolution* **4**:863–869.
- 734 Kloos J, Gama JA, Hegstad J, Samuelsen Ø, Johnsen PJ. 2021. Piggybacking on niche-
735 adaptation improves the maintenance of multidrug resistance plasmids. *Mol Biol Evol*.
736 doi:10.1093/molbev/msab091

- 737 Kosterlitz O, Muñoz Tirado A, Wate C, Elg C, Bozic I, Top EM, Kerr B. 2022. Estimating the
738 transfer rates of bacterial plasmids with an adapted Luria-Delbrück fluctuation analysis.
739 *PLoS Biol* **20**:e3001732.
- 740 Lakens D, Scheel AM, Isager PM. 2018. Equivalence Testing for Psychological Research: A
741 Tutorial. *Advances in Methods and Practices in Psychological Science* **1**:259–269.
- 742 Lenth RV. 2023. Estimated Marginal Means, aka Least-Squares Means [R package emmeans
743 version 1.8.9].
- 744 Lilley AK, Bailey MJ, Day MJ, Fry JC. 1996. Diversity of mercury resistance plasmids obtained
745 by exogenous isolation from the bacteria of sugar beet in three successive years. *FEMS*
746 *Microbiol Ecol* **20**:211–227.
- 747 Loftie-Eaton W, Bashford K, Quinn H, Dong K, Millstein J, Hunter S, Thomason MK, Merrikh H,
748 Ponciano JM, Top EM. 2017. Compensatory mutations improve general permissiveness
749 to antibiotic resistance plasmids. *Nat Ecol Evol* **1**:1354–1363.
- 750 Machnicka MA, Kaminska KH, Dunin-Horkawicz S, Bujnicki JM. 2015. Phylogenomics and
751 sequence-structure-function relationships in the GmrSD family of Type IV restriction
752 enzymes. *BMC Bioinformatics* **16**:336.
- 753 Mei H, Arbeithuber B, Cremona MA, DeGiorgio M, Nekrutenko A. 2019. A High-Resolution View
754 of Adaptive Event Dynamics in a Plasmid. *Genome Biol Evol* **11**:3022–3034.
- 755 Payne LJ, Todeschini TC, Wu Y, Perry BJ, Ronson CW, Fineran PC, Nobrega FL, Jackson SA.
756 2021. Identification and classification of antiviral defence systems in bacteria and
757 archaea with PADLOC reveals new system types. *Nucleic Acids Res* **49**:10868–10878.
- 758 Porse A, Schønning K, Munck C, Sommer MOA. 2016. Survival and Evolution of a Large
759 Multidrug Resistance Plasmid in New Clinical Bacterial Hosts. *Mol Biol Evol* **33**:2860–
760 2873.
- 761 Prensky H, Gomez-Simmonds A, Uhlemann A-C, Lopatkin AJ. 2021. Conjugation dynamics
762 depend on both the plasmid acquisition cost and the fitness cost. *Mol Syst Biol*
763 **17**:e9913.
- 764 Rebelo JS, Domingues CPF, Dionisio F. 2023a. Plasmid costs explain Plasmid maintenance,
765 irrespective of the nature of compensatory mutations. *Antibiotics (Basel)* **12**:841.
- 766 Rebelo JS, Domingues CPF, Nogueira T, Dionisio F. 2023b. Plasmids increase the competitive
767 ability of Plasmid-bearing cells even when transconjugants are poor donors, as shown
768 by computer simulations. *Microorganisms* **11**:1238.
- 769 San Millan A, MacLean RC. 2017. Fitness Costs of Plasmids: a Limit to Plasmid Transmission.
770 *Microbiol Spectr* **5**. doi:10.1128/microbiolspec.MTBP-0016-2017

771 San Millan A, Toll-Riera M, Qi Q, MacLean RC. 2015. Interactions between horizontally
772 acquired genes create a fitness cost in *Pseudomonas aeruginosa*. *Nat Commun* **6**:6845.
773 Simonsen L, Gordon DM, Stewart FM, Levin BR. 1990. Estimating the rate of plasmid transfer:
774 an end-point method. *J Gen Microbiol* **136**:2319–2325.
775 Stalder T, Rogers LM, Renfrow C, Yano H, Smith Z, Top EM. 2017. Emerging patterns of
776 plasmid-host coevolution that stabilize antibiotic resistance. *Sci Rep* **7**:4853.
777 Stevenson C, Hall JPJ, Harrison E, Wood A, Brockhurst MA. 2017. Gene mobility promotes the
778 spread of resistance in bacterial populations. *ISME J* **11**:1930–1932.
779 Tesson F, Hervé A, Mordret E, Touchon M, d’Humières C, Cury J, Bernheim A. 2022.
780 Systematic and quantitative view of the antiviral arsenal of prokaryotes. *Nat Commun*
781 **13**:2561.
782 Turner PE, Cooper VS, Lenski RE. 1998. Tradeoff Between Horizontal and Vertical Modes of
783 Transmission in Bacterial Plasmids. *Evolution* **52**:315–329.
784 Turner PE, Williams ESCP, Okeke C, Cooper VS, Duffy S, Wertz JE. 2014. Antibiotic resistance
785 correlates with transmission in plasmid evolution. *Evolution* **68**:3368–3380.
786 Vos M, Padfield D, Quince C, Vos R. 2023. Adaptive radiations in natural populations of
787 prokaryotes: innovation is key. *FEMS Microbiol Ecol*. doi:10.1093/femsec/fiad154
788 Wein T, Dagan T. 2020. Plasmid evolution. *Curr Biol* **30**:R1158–R1163.
789 Zwanzig M, Harrison E, Brockhurst MA, Hall JPJ, Berendonk TU, Berger U. 2019. Mobile
790 Compensatory Mutations Promote Plasmid Survival. *mSystems* **4**:e00186-18.
791
792